Separation Science and Technology
Publication details, including instructions for authors and subscription information:
http://www.informaworld.com/smpp/title~content=t713708471

Kinetic Study of Sr^{2+} Sorption by Bone Char

Slavko Dimović[a]; Ivana Smičiklas[a]; Ilija Plećaš[a]; Dušan Antonović[b]
[a] The Institute of Nuclear Sciences "Vinca", Belgrade, Serbia [b] Faculty of Technology and Metallurgy, Belgrade, Serbia

Online publication date: 22 June 2010

To cite this Article Dimović, Slavko , Smičiklas, Ivana , Plećaš, Ilija and Antonović, Dušan(2009) 'Kinetic Study of Sr^{2+} Sorption by Bone Char', Separation Science and Technology, 44: 3, 645 — 667
To link to this Article: DOI: 10.1080/01496390802634307
URL: http://dx.doi.org/10.1080/01496390802634307

Separation Science and Technology, 44: 645–667, 2009

ISSN: 0149-6395 print/1520-5754 online
DOI: 10.1080/01496390802634307

Taylor & Francis
Taylor & Francis Group

Kinetic Study of Sr^{2+} Sorption by Bone Char

Slavko Dimović,[1] Ivana Smičiklas,[1] Ilija Plećaš,[1] and Dušan Antonović[2]
[1]The Institute of Nuclear Sciences "Vinca", Belgrade, Serbia
[2]Faculty of Technology and Metallurgy, Belgrade, Serbia

Abstract: The effect of particle size, bone char mass, initial pH, and metal concentration on the kinetics of Sr^{2+} sorption by bone char was studied and discussed. Considering the sorbed amounts of Sr^{2+}, solution pH changes, changes of Ca^{2+} concentrations and Ca/Sr molar ratios, with time, it was concluded that surface complexation reactions are dominant in the first, more rapid stage of the sorption process, while the contribution of the ion-exchange mechanism increases with time and becomes more significant in the second, slower phase. Under all investigated experimental conditions, the pseudo-second-order model was found to provide high correlation coefficients and the equilibrium amounts of Sr^{2+} sorbed comparable to the values obtained experimentally.

Keywords: Bone char, kinetic models, sorption kinetics, Sr^{2+}

INTRODUCTION

Strontium is the fifteenth most abundant element on earth that is commonly found in nature in the form of the sulfate mineral celestite ($SrSO_4$) and the carbonate strontianite (SrO_3) (1). It has 16 known isotopes: four of them are stable while twelve others are radioactive. As a metal, strontium is used in the production of glass for color television tubes and ferrite magnets, while its salts are used for the production of optical

Received 22 February 2008; accepted 18 August 2008.
Address correspondence to Slavko Dimović, The Institute of Nuclear Sciences, "Vinca", P.O. Box 522, Belgrade, Serbia. Tel.: +381 11 8066 439; Fax: +381 11 2455 943. E-mail: sdimovic@vin.bg.ac.yu

materials. Radioactive isotope ^{90}Sr (beta emitter; $t_{1/2}$ 28 y) is used as a radioactive tracer in medical and agricultural studies, as a radiation source in industrial thickness gauges, and for the treatment of eye diseases and bone cancer.

^{90}Sr is also one of the most important radioactive isotopes in the environment that originates as a by-product of the fission of uranium and plutonium in nuclear reactors and in nuclear weapons and enters the environment via above ground nuclear testing, nuclear plant accidents, and leakage from radioactive waste sites (2).

Due to the elements being sufficiently similar chemically, the human body absorbs strontium as if it was calcium. It is rapidly absorbed from the gastrointestinal tract or the lungs into the bloodstream and is subsequently deposited in bones (3). While stable strontium is considered relatively nontoxic to humans (4), ^{90}Sr, known as a ''bone-seeker'', (5,6) becomes a continuing source of ionizing radiation and may cause anemia and oxygen shortages, and at extremely high concentrations it is even known to cause bone cancer and leukemia.

The sorption studies of Sr^{2+} are fundamental for nuclear waste management and environmental protection, therefore different sorbents have been considered for Sr^{2+} immobilization: bentonite (7), kaolinite (8) zeolite (9,10), ferric oxide (11,12), tobermorite (13), hydroxyapatite (14,15), goethite (16), etc.

During the past ten years extensive research has been carried out to find low-cost, high capacity sorbents of biological origin for the removal of metal ions. One of them is bone char—a mixed compound sorbent produced from the destructive distillation of dried, crushed animal bones in which carbon is distributed throughout a porous structure of poorly crystalline hydroxyapatite ($Ca_{10}(PO_4)_6(OH)_2$ or CaHAP) (17). The main cation removal mechanisms by CaHAP are recognized to be ion-exchange reaction with calcium ions of the apatites, dissolution of CaHAP followed by the precipitation of metal-containing phosphate phases, and specific cation sorption on the CaHAP surface (18). While CaHAP has a good ability to remove inorganic cations (and in a lesser extent anions) the carbon component of the bone char can also remove some organic components.

Traditionally bone char has been used to decolorize sugar solutions in the sugar refining industry and for fluoride anion removal from aqueous solutions (19). More recently it has been studied as an immobilization agent for heavy metals such as Cu^{2+}, Cd^{2+} and Zn^{2+} (20–23) and radionuclides: $^{124}Sb^{3+}$, $^{124}Sb^{5+}$, $^{152}Eu^{3+}$ (24), as well as U(VI) (25). Bone char was also found to be a promising additive for the reduction of bioavailability of Pb^{2+} in a polluted soil, through transformation of soil Pb^{2+} from non-residual to the residual fraction (17).

The good retention properties of bones towards ^{90}Sr ions, which cause health problems in humans, represent, on the other hand, a benefit in respect to ^{90}Sr removal from aqueous media by bone based sorbents. In our previous study the maximum sorption capacity of bone char towards Sr^{2+} was found to be 0.273 mmol/g, which is higher in respect to various low-cost sorbents. The influence of pH on the sorption was studied as well as the influence of pH and Ca^{2+} content on Sr^{2+} desorption from bone char surface (26).

While sorption equilibrium studies provide valuable information about sorption capacities, the sorption kinetic describes reaction pathways. In the literature a great deal of attention has been paid in order to clarify the kinetics of heavy metal cations sorption by bone char (20,27–29), whereas no data exist on Sr^{2+} sorption kinetics.

The main objectives of the present study were:

1. to investigate the effects of various sorption parameters (initial concentration of Sr^{2+}, bone char particles size, bone char mass, and solution pH) on the kinetics of Sr^{2+} immobilization by bone char,
2. to evaluate main sorption mechanisms, based on the solution pH changes, Sr^{2+} and Ca^{2+} concentrations changes as a function of time, and
3. to test different theoretical models and compare their applicability regarding investigated system.

MATERIALS AND METHODS

Bone Char

The bone char used in this study was supplied by Imperial-Oel-Import. The physical and chemical properties of the sample were provided by the manufacturer (Table 1). The point of zero charge (pH_{PZC}) of bone char, determined by batch equilibration technique, using 0.1 mol/dm^3 KNO_3 as inert electrolyte, was found to be 8.4 (26).

Furthermore, the sorbent was analyzed by X-ray diffraction (XRD), using a Philips PW 1050 diffraction system, with Cu$K\alpha_{1,2}$ Ni-filtrated radiation. The patterns were registered in the 2θ range 10–100° with a scanning step size of 0.02°.

Prior to sorption experiments, bone char was rinsed with distilled water, dried at 105°C for 24 h, and then allowed to cool in the desiccator. The dried sorbent was then milled and sieved into different particle sizes.

Table 1. Physico-chemical properties of bone char (source: Imperial-Oel-Import)

Chemical composites	Limits (wt.%)
Acid insoluble ash	≤ 3
Calcium carbonate	7–9
Calcium sulphate	0.1–0.2
Carbon	8–11
Iron as Fe_2O_3	≤ 0.3
Total phosphate as P_2O_5	30
Water soluble phosphate as P_2O_5	0.003
Phosphate soluble in 2% citric acid	16.5
Hydroxyapatite	70–76
Physical properties	
Moisture	≤ 5 wt.%
Total surface area	80–120 m^2/g
Carbon surface area	40–60 m^2/g
Pore size distribution	7.5–60 000 nm
Pore volume	0.225 cm^3/g

Sorption Experiments

In order to investigate parameters influencing kinetics of Sr^{2+} immobilization by bone char such as: initial concentration of Sr^{2+}, particles size, bone char mass, and solution pH, sorption experiments were conducted in a controlled batch system. All chemicals were commercial products (p.a.) used without purification. Strontium solutions of desired concentrations were prepared from $Sr(NO_3)_2$ (Merck), by dissolving the exact quantities of strontium salts in distilled water. The initial pH values of the solutions were adjusted by adding 0.01 M HNO_3 or KOH. Particular amounts of sorbent were weighed and put into PVC flasks containing 20.00 ml of desired solution. The PVC flasks with suspensions were placed on a horizontal shaker, and after specified periods of time, ranging from 15 min to 48 h, the sorbent was separated from the solution by filtration through blue-band filter paper (Quant, Grade 391).

Unless a process parameter was the system variable, the following conditions were used: 0.1 g of bone char, bone char particle size 45–250 μm, initial Sr^{2+} concentration 6×10^{-3} mol/dm^3, solution pH 5, agitation speed 120 rpm, and temperature 20°C.

The initial Sr^{2+} concentrations, as well as the Sr^{2+} and Ca^{2+} concentrations after the sorption were determined by a Perkin–Elmer Analyst 200 Atomic Absorption Spectrometer. The flame type was air/acetylene, while absorption wavelengths were 460.7 and 422.7 nm for Sr^{2+} and

Ca^{2+}, respectively. Initial and final pH values were measured with an Inolab, WTW glass electrode pH meter.

The sorbed amounts of Sr^{2+} were calculated from the mass balance equation:

$$q = (\Delta C \cdot V)/M \quad (1)$$

where q (mol/g) is the sorbed amount, ΔC (mol/dm^3) is the difference in Sr^{2+} concentration before and after the experiment, V (dm^3) is the volume of solution and M (g) is the mass of bone char.

RESULTS AND DISCUSSION

Characteristics of Bone Char Sorbent

From Table 1 it can be concluded that the main componsent of bone char is CaHAP (>70 wt.%), while carbon and $CaCO_3$ presents 8–11 and 7–9 wt.%, respectively. However, it should be noted that although present in a relatively small amount, carbon phase has a large specific surface area in respect to the total surface area (40–60 m^2/g vs. 80–120 m^2/g, respectively). The XRD analyses of bone char (Fig. 1) have confirmed that poorly crystalline CAHAP is a main constituent of the inorganic phase. In addition, the presence of β-tri-calcium-phosphate, calcium-carbonate, and a small amount of well crystalline quartz was observed.

Effect of Particle Size

In order to examine the effect of particle size on the sorption process, the dried bone char was crushed and sieved into different size fractions: 45–200, 200–250, 250–300 μm. It was obvious from the result shown in Fig. 2a, that the uptake of Sr^{2+} is a two-step process with initial rapid phase (up to 6 h of contact), followed by a slower uptake. The minor increase of the amount of Sr^{2+} sorbed at equilibrium (from 0.251 to 0.263 mmol/g) was observed, with the bone char particle size decrease, in the investigated range.

The variation in particle size, in the investigated ranges, appeared to have no influence on the time required to reach equilibrium. For all particle sizes the time required to reach equilibrium, at applied experimental conditions, was about 24 h. Using horizontal shaker at 120 rpm

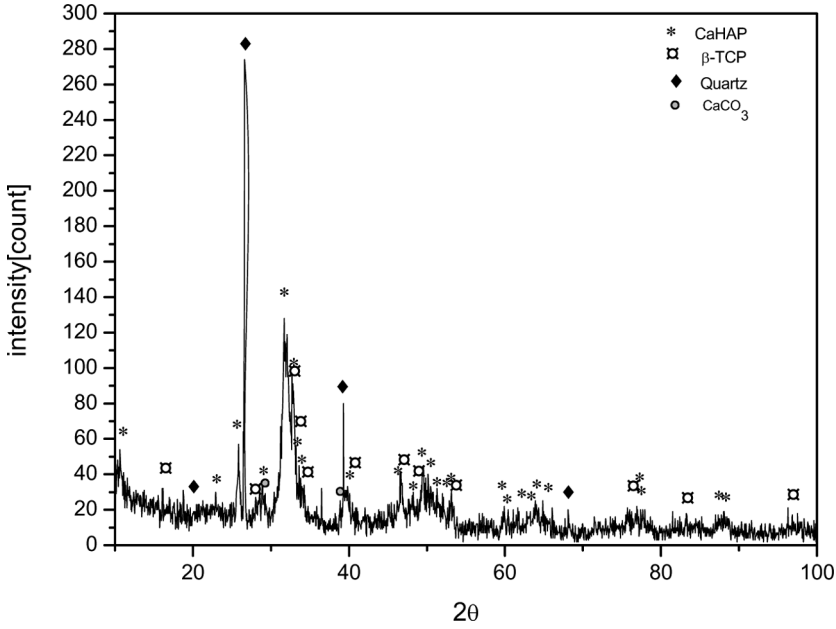

Figure 1. XRD pattern of bone char.

equilibrium times were higher than practical residence times of wastewater treatment processes (usually a few hours). Therefore, optimization of stirring conditions (type of agitation device, agitation speed, etc.) is required, in order to exploit the full sorption capacity of bone char in shorter time periods.

Figure 2b, shows that uptake of Sr^{2+} was followed by release of Ca^{2+} ions from CaHAP phase of bone char, indicating the existence of ion-exchange mechanism. Furthermore, the molar ratio between released and sorbed metal cations as a function of time was calculated and presented in Fig. 2c. This ratio increased with time, for all investigated particle sizes, up to the value of approximately 0.5.

Another significant parameter, related to the sorption mechanism, is solution pH. All initial pH values were adjusted to 5, while final pH values were measured as a function of time and are presented in Fig. 2d. Final pH values generally increased with time, reaching value of approximately 7.3 at equilibrium. However, solution pH after addition of bone char sorbent would increase up to 8.4 (pH_{PZC}) in the absence of Sr^{2+} ions. Solution pH values lower in respect to pH_{PZC} indicated the specific cation sorption, which can be presented by the

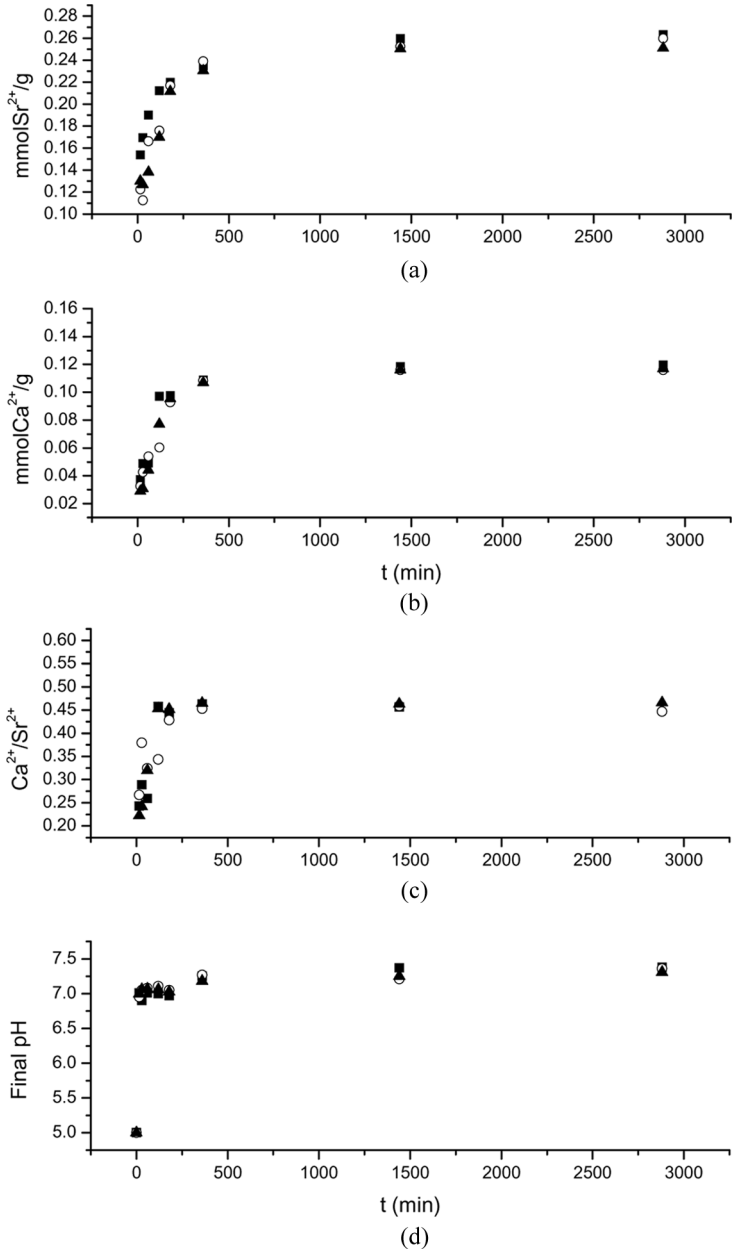

Figure 2. Effect of particle size (■ 45–200 μm, ○ 200–250 μm, ▲ 250–300 μm) on the (a) amount of sorbed Sr^{2+}, (b) amount of Ca^{2+} released, (c) Ca^{2+}/Sr^{2+} molar ratio, (d) final solution pH.

following surface reactions:

$$\equiv POH + Sr^2 = \equiv POSr^+ + H^+ \quad (2)$$

$$\equiv PO^- + Sr^2 = \equiv POSr^+ \quad (3)$$

$$\equiv CaOH + Sr^2 = \equiv CaOSr^+ + H^+ \quad (4)$$

$$\equiv COOH + Sr^2 = \equiv COOSr^+ + H^+ \quad (5)$$

where equations 2–5 describe reactions between Sr^{2+} from the solution with CaHAP and carbon phase surface groups, respectively.

On the basis of the sorbed amounts of Sr^{2+}, solution pH changes, changes of Ca^{2+} concentrations and Ca/Sr molar ratios, with time, it could be concluded that surface reactions (Eqs. 10–13) were dominant in the first stage of the sorption process, while the contribution of the ion-exchange mechanism became more significant after 6 h of contact. Considering Ca/Sr molar ratios at equilibrium, it was evident that about 50% of sorbed Sr^{2+} replaced Ca^{2+} in the inorganic phase of bone char.

Effect of Bone Char Mass

The effect of different bone char mass on the sorption of Sr^{2+} was investigated for the doses of 0.1 g, 0.2 g, 0.3 g, and 0.5 g in 20 ml of Sr^{2+} solution. It was noticed that although the total amount of Sr^{2+} removed from the solution was higher when the bone char mass increased, the removed amount calculated per 1 g of sorbent decreased from 0.263 to 0.147 mmol/g (Fig. 3a). Factors that could have contributed to this adsorbent concentration effect might have been a shortage of metal concentration in solution and a lower adsorptive capacity utilization for higher concentrations of a sorbent, i.e. unsaturation of sorption sites (30).

Variations in bone char mass have showed the influence on the time required to reach equilibrium: approximately 24 h was sufficient for lower sorbent doses (0.1 and 0.2 g) while for higher doses (0.3 and 0.5 g) a slight increase of sorbed Sr^{2+} was detected between 24 and 48 h.

The plots of Ca^{2+} released and Ca/Sr molar ratios as a function of time, for different bone char doses, are presented in Figs. 3b and 3c. The amounts of Ca^{2+} released increased with time and with the decrease of the amount of sorbent added, following the shape of Sr^{2+} sorption curves. The Ca/Sr molar ratios increased with time emphasizing the role of ion-exchange mechanism in the second sorption step, but they were

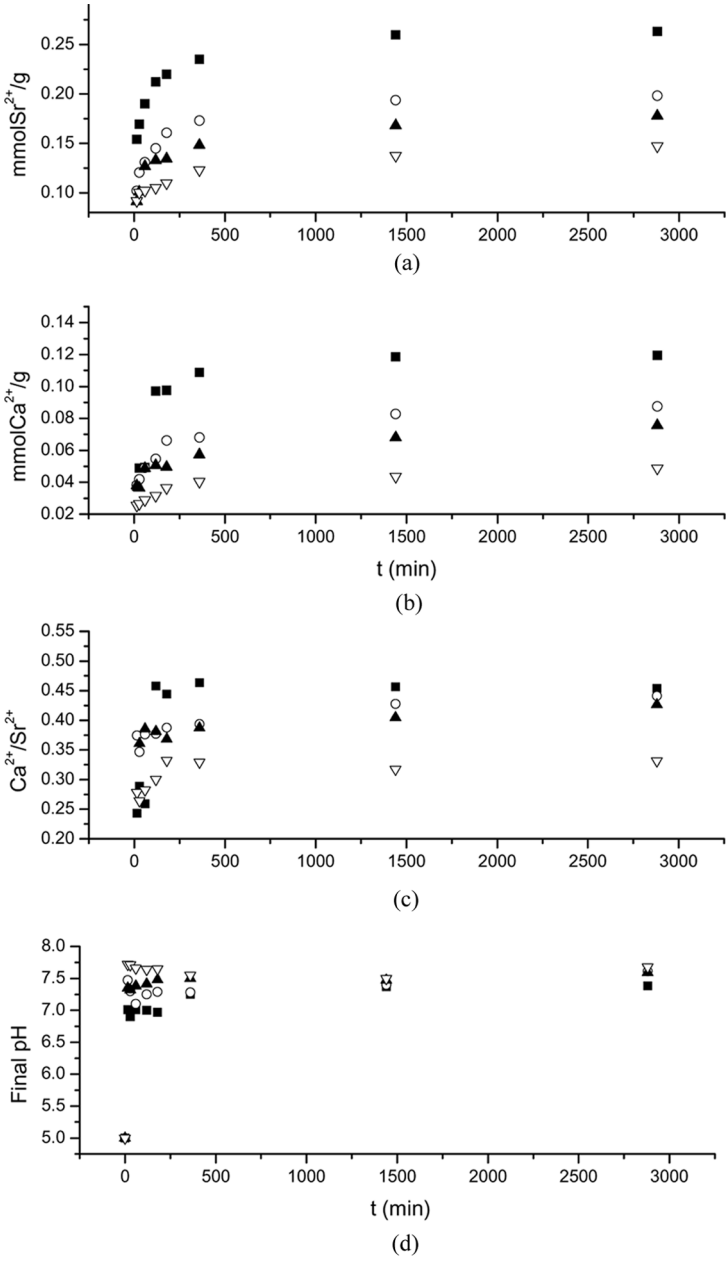

Figure 3. Effect of sorbent mass (■, 0.1 g, ○, 0.2 g, ▲, 0.3 g, ▽, 0.5 g) on the (a) amount of sorbed Sr^{2+}, (b) amount of Ca^{2+} released, (c) Ca^{2+}/Sr^{2+} molar ratio, (d) final solution pH.

generally lower for higher bone char doses. The increase of final solution pH (Fig. 3d) with the increase of bone char mass, was more obvious in the first, more rapid step of Sr^{2+} sorption, while the differences became minor as the process reached equilibrium. The explanation may be found in lower Sr^{2+} sorption capacity utilization at higher mass dosages, resulting in more functional groups on the bone char surface available for interaction with solution H^+ ions. Consequently, at higher sorbent concentrations final pH values were closer to pH_{PZC}.

Effect of Initial Metal Concentration

The effect of the initial Sr^{2+} concentration on the rate of sorption was studied using solutions of 1×10^{-4}, $1\times s10^{-3}$, 3×10^{-3}, and 6×10^{-3} molSr^{2+}/dm^3. These results are presented in Fig. 4.

The necessary time to reach the equilibrium was a variable of the initial concentration of Sr^{2+} (Fig. 4a): approximately 24 h for 6×10^{-3} mol/dm^3, 6 h for 3×10^{-3} mol/dm^3, and approximately 3 h for 1×10^{-3} mol/dm^3 and 10^{-4} mol/dm^3.

The sorption capacity at equilibrium increased from 0.0195 to 0.2633 mmol/g with an increase in the Sr^{2+} concentration from 1×10^{-4} to 6×10^{-3} mol/dm^3.

The amounts of Ca^{2+} released, as well as molar Ca/Sr ratios (Figs. 4b and 4c) increased both with the increase of contact time and the increase of Sr^{2+} concentration. This is another clear indication of the participation of an ion-exchange mechanism.

Figure 4d shows sharp final pH increase, at the beginning of the sorption process, governed by the buffering capacity of the sorbent. However, the final pH values at high sorbate concentrations were lower compared to solutions of low Sr^{2+} concentration, confirming the increase of specific cation sorption contribution with the overall increase of the amount of Sr^{2+} sorbed. Equilibrium pH values decreased from 7.9 to 7.38 with increasing Sr^{2+} concentration from 10^{-4} to 6×10^{-3} mol/dm^3.

The observed phenomena were consistent with the reported results on concentration dependant Cu^{2+} and Cd^{2+} sorption onto bone char (27,31) where the ion-exchange rate of sorption was also found to increase with time.

Effect of Initial pH

In order to avoid dissolution of the major constituent of bone char, CaHAP, at pH<5 (32), and taking into account bone char large buffering

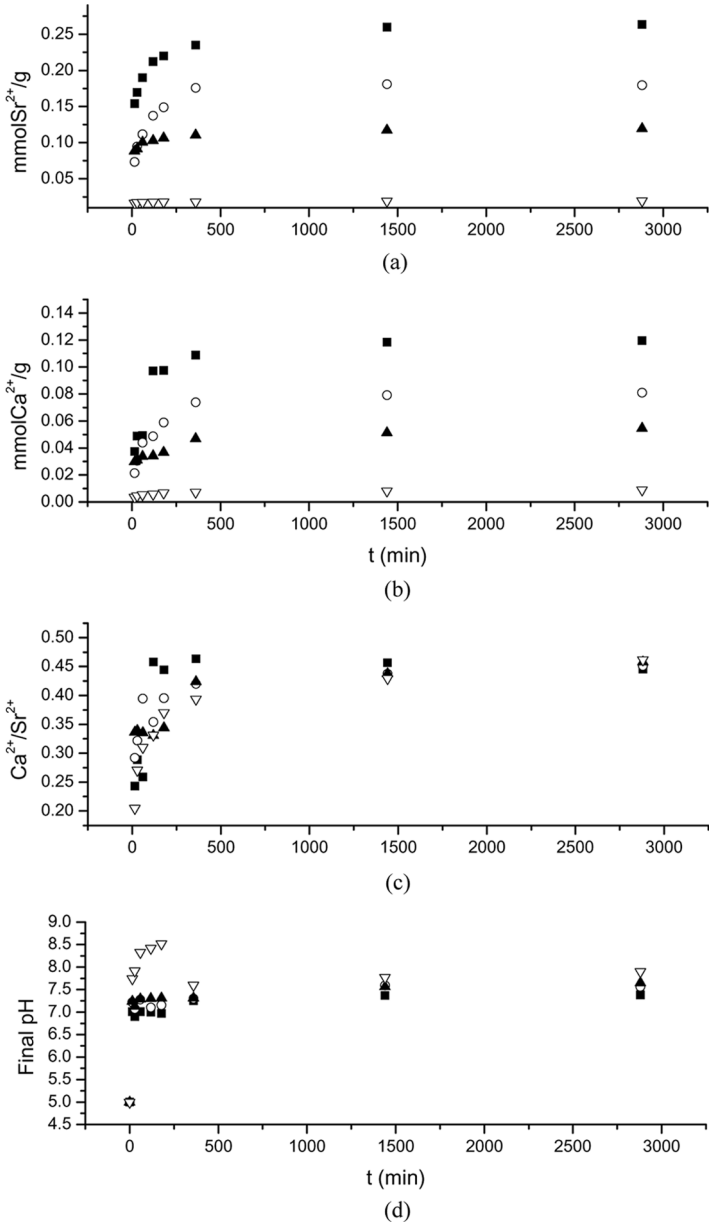

Figure 4. Effect of initial Sr^{2+} concentration (■, $6{\cdot}10^{-3}$ mol/dm^3, ○, $3{\cdot}10^{-3}$ mol/dm^3, ▲, 10^{-3} mol/dm^3, ▽, 10^{-4} mol/dm^3) on the (a) amount of sorbed Sr^{2+}, (b) amount of Ca^{2+} released, (c) Ca^{2+}/Sr^{2+} molar ratio, (d) final solution pH.

capacity (26), the influence of the initial pH of the solution on the Sr^{2+} uptake was studied at pH values 5, 7, and 12. These results are presented in Fig. 5.

The sorption capacity of bone char towards Sr^{2+}, at equilibrium, increased from 0.2633 to 0.8845 mmol/g with an increase of the initial pH from 5 to 12 (Fig. 5a). Furthermore, there was only a slight difference between sorption at pH 5 and pH 7. It was also noticed that the variation in initial pH of the solution had no influence on the time required to reach equilibrium (for all initial pH the time required to reach equilibrium is about 24 h).

On the other hand, the amounts of Ca^{2+} released increased with time, but decreased with the increase of initial pH (Fig. 5b). The same relationships were observed for Ca/Sr molar ratios (Fig. 5c). These results can be explained by the increased CaHAP stability with the increase of solution pH (33), meaning that substitution of Ca^{2+} with Sr^{2+} was unfavorable process at elevated pH.

Figure 5d. shows the relationship between final pH values and time. For initial pH 5 and 7, final pH changes with time were almost the same, which explains the similarity between amounts of Sr^{2+} sorbed and Ca^{2+} released. Conversely, for initial pH 12, the final pH values increased up to 11.2. Since Sr^{2+} ions do not hydrolyze in the investigated pH range, higher Sr^{2+} uptake at elevated pH can be explained by alteration of bone char surface charge. At elevated pH, the sorption of the OH^- species on the surface of the bone char resulted in the appearance of negative surface charge which promoted cation sorption. The similar increase of Sr^{2+} sorption in alkaline environment was obtained using synthetic CaHAP (15).

Modeling of Kinetic Data

Three simplified kinetic models including a pseudo-first-order, pseudo-second-order, and intraparticle diffusion model were selected to follow the sorption process of Sr^{2+} by bone char, at different experimental condition.

A pseudo-first-order kinetic model proposed by Lagergreen (34) and the pseudo-second-order model derived by Ho and McKay (35) can be presented in linear forms by equations 6 and 7, respectively:

$$\log(q_l - q_t) = \log q_l - \frac{k_1}{2.303} t \tag{6}$$

$$\frac{t}{q_t} = \frac{1}{k_2 q_2^2} + \frac{1}{q_2} t \tag{7}$$

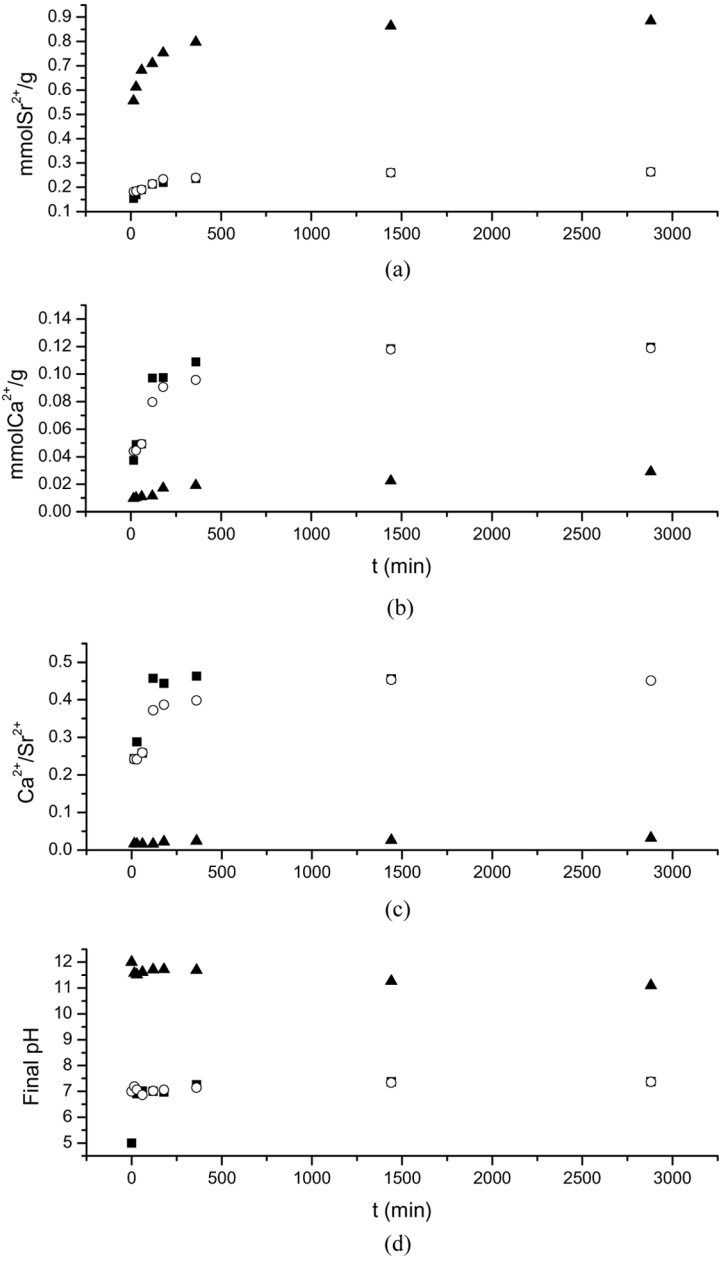

Figure 5. Effect of initial pH (■, pH 5, ○, pH 7, ▲, pH 12) on the (a) amount of sorbed Sr^{2+}, (b) amount of Ca^{2+} released, (c) Ca^{2+}/Sr^{2+} molar ratio, (d) final solution pH.

where q_1 and q_2 (mmol/g) are the amounts of Sr^{2+} sorbed on the surface of the bone char at equilibrium, q_t (mmol/g) is the amount sorbed at any time t, whereas k_1 (min^{-1}) and k_2 (g/mmol min) are the rate constants for pseudo-first and pseudo-second order reactions, respectively.

Kinetic parameters can be calculated from the intercepts and slopes of the lines obtained by plotting $\log(q_1-q_t)$ versus t, and t/q_t versus t. Once the k_2 and q_2 values are calculated, the initial sorption rates h (mmol/g min) can be derived using the following expression:

$$h = k_2 q_2^2 \tag{8}$$

The intraparticle diffusion equation, which refers to the theory proposed by Weber and Morris (36), was considered in order to determine the participation of intraparticle diffusion in the sorption of Sr^{2+} by

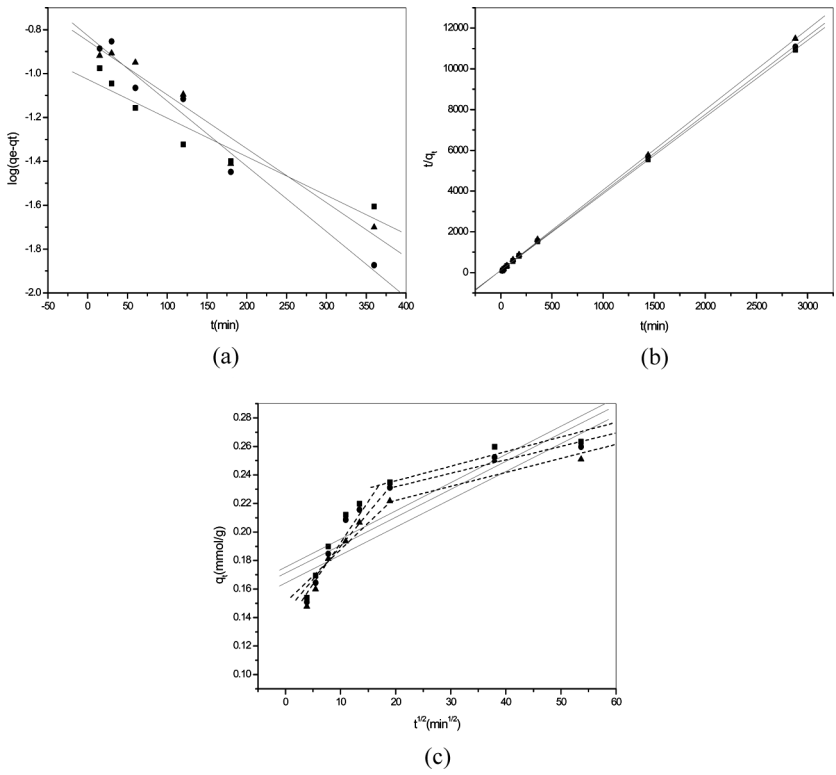

Figure 6. Modeling kinetic data for different particle size (■, 45–200, ●, 200–250 and ▲, 250–300 μm) using: (a) pseudo-first-order, (b) pseudo-second-order and (c) intraparticle diffusion model.

bone char. The rate parameter for intraparticle diffusion, k_{int}, can be defined as:

$$q_t = k_{int} t^{1/2} \tag{9}$$

where k_{int} is the intraparticle rate constant (mmol/g $min^{0.5}$). According to this model, the plot of uptake, q_t versus the square root of time, should be linear if intraparticle diffusion is involved in the sorption process. If these lines pass through the origin then the intraparticle diffusion is the rate controlling step. Furthermore, such plots may also demonstrate a multilinearity (37), signifying that two or more steps take place.

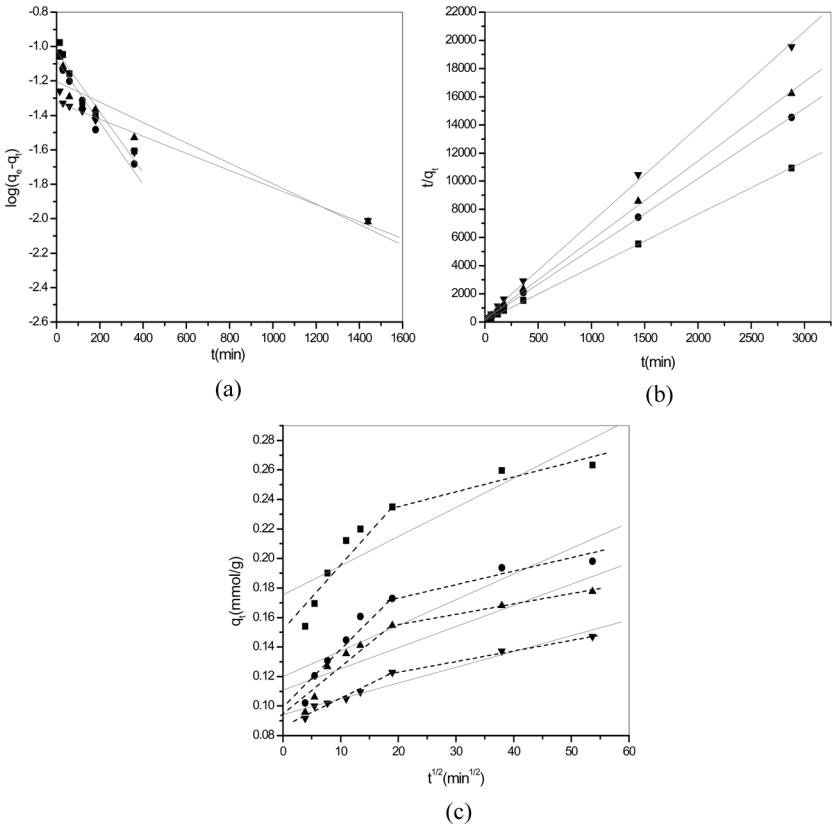

Figure 7. Modeling kinetic data for different sorbent masses (■, 0.1 g, ●, 0.2 g, ▲, 0.3 g and ▼, 0.5 g) using: (a) pseudo-first-order, (b) pseudo-second-order and (c) intraparticle diffusion model.

The linear data fitting using different theoretical models is presented in Figs. 6–9, while calculated kinetic parameters and corresponding correlation coefficients are listed in Tables 2–4.

For all kinetic parameters the values of r_2^2 of pseudo-second-order kinetic model for Sr^{2+} sorption were extremely high (Table 3) and were followed by the values of pseudo-first-order r_1^2 (Table 2) and intraparticle diffusion equation, r_{int} (Table 4). Moreover, the equilibrium sorption capacities predicted by the pseudo second-order model were very close to $q_{e,exp.}$, while q_1 values of pseudo-first-order model were 2–10 times lower. Therefore, even though the values of ${r_1}^2$ were relatively high, sorption of Sr^{2+} by bone char did not follow a first-order kinetics model. A

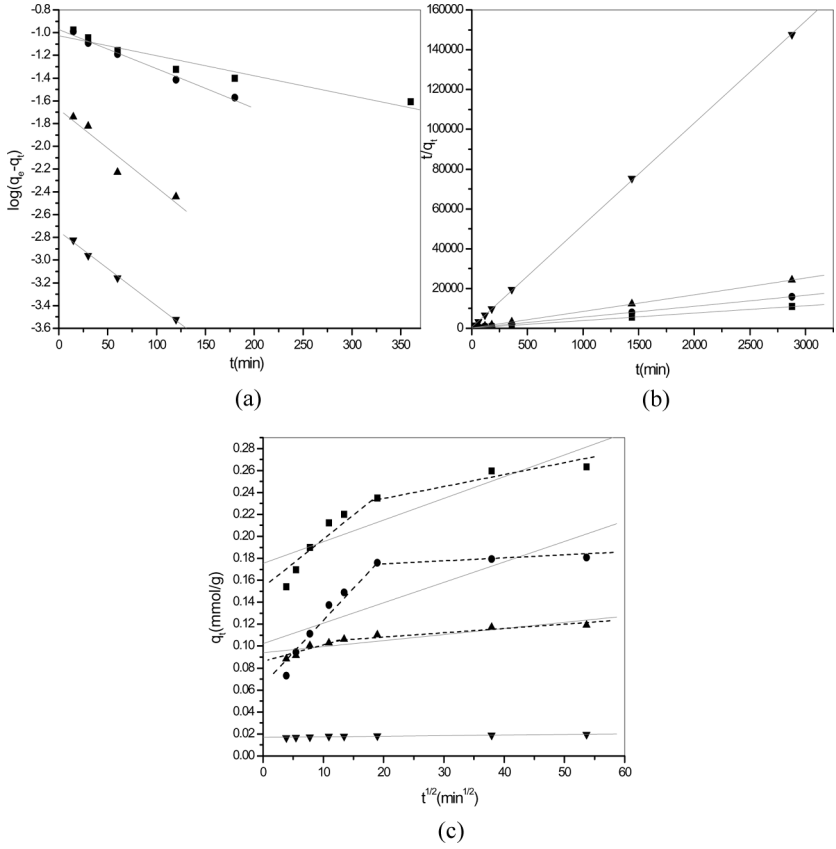

Figure 8. Modeling kinetic data for different Sr^{2+} concentrations (▼, 10^{-4}, ▲, 10^{-3} ●, 3×10^{-3} and ■, 6×10^{-3} mol/dm^3) using: (a) pseudo-first-order, (b) pseudo-second-order and (c) intraparticle diffusion model.

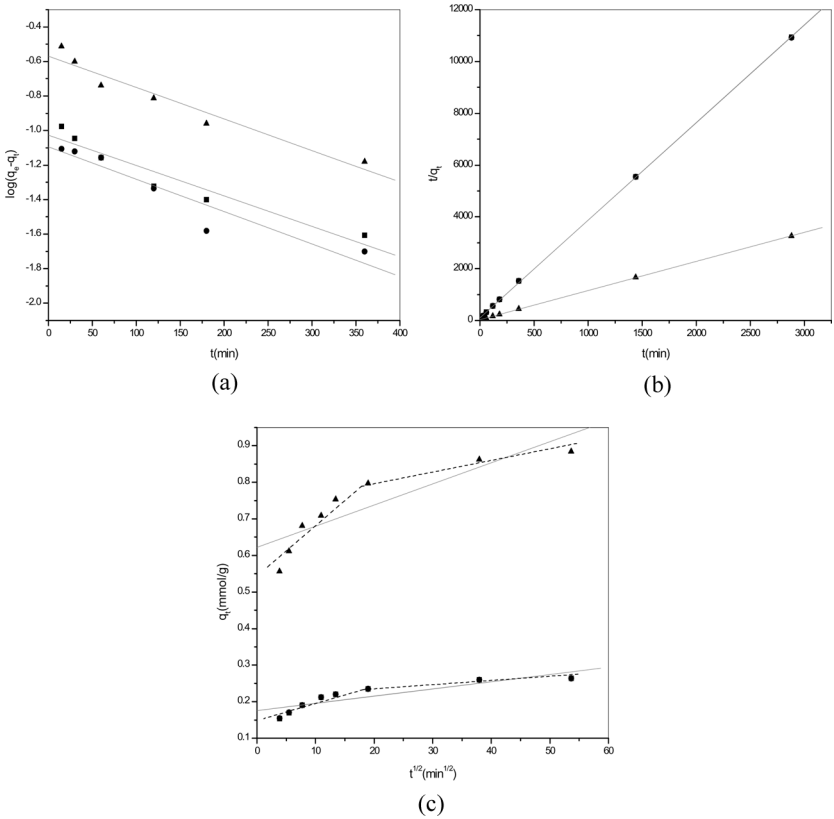

Figure 9. Modeling kinetic data for different initial pH (■, 5, ●, 7 and ▲, 12) using: (a) pseudo-first-order, (b) pseudo-second-order and (c) intraparticle diffusion model.

good correlation with the pseudo-second-order model was also reported for Sr^{2+} sorption by synthetic CaHAP (15), zeolite (9,10) tobermorite (13), and brewery's waste biomass (38). A good correlation between experimental data and a pseudo-second-order kinetic model is principally useful for the purpose of comparison and q_e prediction, whereas deriving conclusions on actual sorption mechanism is difficult taking into account that sorption processes which were found to obey this model, include different sorption mechanisms and their combinations, (such as ion-exchange, surface complexation and dissolution/precipitation (39–41).

The pseudo-second-rate constants were the most affected by alkaline conditions and by variation of sorbent/sorbate ratio (Table 3). In pH interval 5–7 the pseudo second-order rate constants and initial sorption

Table 2. Pseudo-first-order kinetic equation parameters

Variable	Pseudo first-order kinetic equation			
	$q_{e,exp}$ (mmol/g)	q_1 (mmol/g)	$k_1 \cdot 10^3$ (min^{-1})	r_1^2
45–200 μm	0.260	0.093	4.03	0.924
200–250 μm	0.252	0.149	6.84	0.973
250–300 μm	0.250	0.141	5.67	0.959
0.1 g	0.260	0.093	4.03	0.924
0.2 g	0.194	0.083	4.14	0.953
0.3 g	0.178	0.063	1.37	0.903
0.5 g	0.147	0.048	1.14	0.953
$1 \cdot 10^{-4}$ mol/dm^3	0.018	0.002	15.04	0.996
$1 \cdot 10^{-3}$ mol/dm^3	0.106	0.021	15.80	0.916
$3 \cdot 10^{-3}$ mol/dm^3	0.176	0.107	7.99	0.987
$6 \cdot 10^{-3}$ mol/dm^3	0.260	0.093	4.03	0.924
pH = 5	0.260	0.093	4.03	0.924
pH = 7	0.264	0.081	4.33	0.904
pH = 12	0.863	0.270	4.19	0.939

rates remained almost even, whereas at initial pH 12 decreased and increased respectively. This was a confirmation of different sorption mechanism of Sr^{2+} at elevated pH. The much faster initial sorption rate

Table 3. Pseudo-second-order kinetic equation parameters

Variable	Pseudo second-order kinetic equation			
	q_2 (mmol/g)	k_2 (g/mmol·min)	$h \cdot 10^2$ (mmol/g·min)	r_2^2
45–200 μm	0.265	0.137	0.963	0.999
200–250 μm	0.261	0.130	0.886	0.999
250–300 μm	0.254	0.136	0.874	0.999
0.1 g	0.265	0.137	0.963	0.999
0.2 g	0.200	0.139	0.557	0.999
0.3 g	0.178	0.152	0.483	0.999
0.5 g	0.148	0.155	0.339	0.998
$1 \cdot 10^{-4}$ mol/dm^3	0.019	4.296	0.163	0.999
$1 \cdot 10^{-3}$ mol/dm^3	0.119	0.495	0.707	0.999
$3 \cdot 10^{-3}$ mol/dm^3	0.183	0.178	0.597	0.999
$6 \cdot 10^{-3}$ mol/dm^3	0.265	0.137	0.963	0.999
pH = 5	0.265	0.137	0.963	0.999
pH = 7	0.266	0.137	0.964	0.999
pH = 12	0.889	0.0445	3.513	0.999

Table 4. Intraparticle diffusion kinetic equation parameters

Variable	Intraparticle diffusion equation	
	$k_{int} \cdot 10^3$ (mmol/g·min$^{1/2}$)	r_{int}^2
45–200 μm	1.977	0.770
200–250 μm	1.960	0.771
250–300 μm	1.952	0.805
0.1 g	1.977	0.770
0.2 g	1.740	0.794
0.3 g	1.434	0.791
0.5 g	1.069	0.947
$1 \cdot 10^{-4}$ mol/dm^3	0.053	0.876
$1 \cdot 10^{-3}$ mol/dm^3	0.554	0.779
$3 \cdot 10^{-3}$ mol/dm^3	1.860	0.638
$6 \cdot 10^{-3}$ mol/dm^3	1.977	0.770
pH = 5	1.977	0.770
pH = 7	1.968	0.770
pH = 12	5.782	0.784

at pH 12 was a result of electrostatic attraction forces that occurred between negatively charged sorbent and Sr^{2+} ions. For example, the same electrostatic forces were found to be responsible for the increase of initial sorption rate in disperse dyes/alunite system (42).

Generally, the values of k_2 increased while the initial sorption rates h decreased with a decrease of initial Sr^{2+} concentration as well as with the increase of bone char mass (Table 3). The decrease of Sr^{2+} concentration and increase of bone char mass both resulted in an increase of a sorbent/sorbate ratio, i.e. increase of surface area and number of available sites for sorption. The similar trends in k_2 and h changes with the variation of sorbent dose and sorbate concentration were reported for other sorption systems (43,44). The variation of particle sizes in the investigated range did not cause noticeable effect on the pseudo-second-order rate constant, while the initial sorption rates slightly increased with a decrease of the bone char particle size (Table 3), which was also a result of the larger surface area of smaller particles per same mass of sorbent.

For all investigated kinetic parameters, the intraparticle diffusion model has shown the lowest correlation with experimental data considering the overall reaction period (Table 4). These results suggested that intraparticle diffusion was not a controlling step in Sr^{2+} sorption by bone char. Furthermore, owing to the varying extent of sorption in the initial and final stages of the experiment, plots of q_t versus $t^{0.5}$ could be divided into two straight lines with different slopes (dashed lines in Figs. 6c, 7c,

8c, and 9c.) signifying that two types of mechanisms were operating in the removal of Sr^{2+}. At the beginning of sorption there was a linear region representing the more rapid surface loading, followed by the second linear region representing pore diffusion (30). The intraparticle diffusion step took place after approximately 360 min, except for lower Sr^{2+} concentrations (10^{-3} and 10^{-4} mol/dm^3) where initial surface loading was finished after 180 min. However, intraparticle diffusion still was not the controlling step because the lines did not pass through the origin of the graphs.

CONCLUSIONS

Bone char is a heterogeneous sorbent, composed mainly of carbon and CaHAP, and therefore capable for both physical and chemical sorption. The kinetics of Sr^{2+} sorption by bone char was influenced by the variation of process parameters. The amounts of Sr^{2+} sorbed per 1 g of bone char, at equilibrium, increased with the increase of initial Sr^{2+} concentration and pH, and decreased with the increase of bone char particle size and bone char mass. Equilibrium times depended on concentration and bone char dose (increase with the increase of Sr^{2+} concentration and increase of bone char dose) while other parameters, in the investigated ranges, appeared to have no influence. Surface complexation reactions were found to be responsible for the first, rapid sorption step, while the role of the ion-exchange mechanism became more important in the second, slower phase.

Comparing different kinetic models, under all investigated experimental conditions the overall sorption process was best described by the pseudo-second-order model. The same model was also successfully used for the calculation of the amounts of Sr^{2+} sorbed by bone char, at equilibrium.

Under experimental conditions applied in this study equilibrium times are higher than practical residence times of wastewater treatment processes (usually a few hours). Therefore, optimization of stirring conditions (type of agitation device, agitation speed, etc.) is required, in order to exploit the full sorption capacity of bone char in shorter time periods.

ACKNOWLEDGEMENTS

This work was supported by the Ministry of Science and Environmental Protection of the Republic of Serbia, under Project No. 142050.

REFERENCES

1. Martinez, A.L.; Uribe, A.S. (1995) Interfacial properties of celestite and strontianite in aqueous solutions. *Miner. Eng.*, *8*: 1009.
2. NCRP, National Council on Radiation Protection andMeasurements. (1991) *Some Aspects of Strontium Radiobiology*; NCRP, Bethesda, Maryland.
3. Hobbs, C.H.; McClellan, R.O. (1986) Toxic effects of radiation and radioactive materials. In: *Casarett and Doull's Toxicology: The Basic Science of Poisons*, C.D. Klaassen et al. eds.; Macmillan Publishing Co., Inc.: New York, 669.
4. U. S. Environmental Protection Agency (EPA). (1988) *Drinking Water Criteria Document for Stable Strontium*; ECAO-CIN-DO11, Environmental Criteria and Assessment Office, Cincinnati, OH.
5. Papworth, D.G.; Vennart, J. (1984) The uptake and turnover of ^{90}Sr in the human skeleton. *Phys. Med. Biol.*, *29*: 1045.
6. Lagett, R.W.; Eckerman, K.F.; Williams, L.R. (1982) Strontium-90 in bone: A case study in age-dependent dosimetric modeling. *Health. Phys.*, *43*: 307.
7. Ali Khan, S.; Riaz-ur-Rehman.; Ali Khan, M. (1995) Sorption of strontium on bentonite. *Waste Manage.*, *15*: 641.
8. Yoo, J.; Shinagawa, T.; Wood, J.P.; Linak, W.P.; Santoianni, D.A.; King, C.J.; Seo, Y.; Wendt, J.O.L. (2005) High-temperature sorption of cesium and strontium on dispersed kaolinite powders. *Environ. Sci. Technol.*, *39*: 5087.
9. Abd El-Rahman, K.M.; El-Sourougy, M.R.; Abdel-Monem, N.M.; Ismail, I.M. (2006) Modeling the sorption kinetics of cesium and strontium ions on zeolite A. J. *Nuclear Radiochem. Sci.*, *7*: 21.
10. Smiciklas, I.; Dimovic, S.; Plecas, I. (2007) Removal of Cs^{1+}, Sr^{2+} and Co^{2+} from aqueous solutions by adsorption on natural clinoptilolite. *Appl. Clay Sci.*, *35*: 139.
11. Axe, L.; Anderson, P.R. (1997) Experimental and theoretical diffusivities of Cd and Sr in hydrous ferric oxide. *J Colloid Interface Sci.*, *185*: 436.
12. Hofmann, A.; van Beinum, W.; Meeussen, J.C.; Kretzschmar, R. (2005) Sorption kinetics of strontium in porous hydrous ferric oxide aggregates II. Comparison of experimental results and model predictions. *J. Colloid Interface Sci.*, *283*: 29.
13. Coleman, N.J.; Brassington, D.S.; Raza, A.; Mendham, A.P. (2006) Sorption of Co^{2+} and Sr^{2+} by waste-derived 11 Å tobermorite. *Waste Manage.*, *26*: 260.
14. Smičiklas, I.; Onjia, A.; Marković, J.; Raičević, S. (2005) Comparison of Hydroxyapatite sorption properties towards cadmium, lead, zinc and strontium ions. *Mater. Sci. Forum*, *494*: 405.
15. Smičiklas, I.; Onjia, A.; Raičević, S.; Janaćković, Dj.; Mitrić, M. (2008) Factors influencing the removal of divalent cations by hydroxyapatite. *J. Hazard. Mater.*, *152*: 876.
16. Masset, S.; Monteil-Rivera, F.; Dupont, L.; Dumonceau, J.; Aplincour, M. (2000) Influence of humic acid on sorption of Co(II), Sr(II), and Se(IV) on goethite. *Agronomie*, *20*: 25.

17. Chen, S.B.; Zhu, Y.G.; Ma, Y.B.; McKay, G. (2006) Effect of bone char application on Pb bioavailability in a Pb-contaminated soil. *Environ. Pollut.*, *139*: 433.
18. Monteil-Rivera, F.; Fedoroff, M. (2002) *Sorption of Inorganic Species on Apatites from Aqueous Solutions, Encyclopedia of Surface and Colloid Science*; Marcel Dekker, INC.: New York, pp. 1–26.
19. Mwaniki, D.L. (1992) Fluoride sorption characteristics of different grades of bone charcoal, based on batch tests. *J. Dent. Res.*, *71*: 1310.
20. Cheung, C.W.; Porter, J.F.; McKay, G. (2001) Sorption kinetic analysis for the removal of cadmium ions from effluents using bone char. *Water Res.*, *35*: 605.
21. Wilson, J.A.; Pulford, I.D.; Thomas, S. (2003) Sorption of Cu and Zn by bone charcoal. *Environ. Geochem. Health*, *25*: 51.
22. Ko, D.C.; Cheung, C.W.; Choy, K.K.; Porter, J.F.; McKay, G. (2004) Sorption equilibria of metal ions on bone char. *Chemosphere*, *54*: 273.
23. Choy, K.K.H.; McKay, G. (2005) Sorption of metal ions from aqueous solution using bone char. *Environ. Int.*, *31*: 845.
24. Abdel Raouf, M.W.; Daifullah, A.A.M. (1997) Potential use of bone charcoal in the removal of antimony and europium radioisotopes from radioactive wastes. *Adsorpt. Sci. Technol.*, *15*: 559.
25. Fuller, C.C.; Bargar, J.R.; Davis, J.A. (2003) Molecular-scale characterization of uranium sorption by bone apatite materials for a permeable reactive barrier demonstration. *Environ. Sci. Technol.*, *37*: 4642.
26. Smičiklas, I.; Dimović, S.; Šljivić, M.; Plećaš, I. (2008) The batch study of Sr^{2+} sorption by bone char. *J. Environ. Sci. Health A*, *48*: 210.
27. Cheung, C.W.; Porter, J.F.; McKay, G. (2000) Sorption kinetics for the removal of copper and zinc from effluents using bone char. *Sep. Purif. Technol.*, *19*: 55.
28. Choy, K.K.H.; McKay, G. (2005) Sorption of cadmium, copper, and zinc ions onto bone char using Crank diffusion model. *Chemosphere*, *60*: 1141.
29. Choy, K.K.H.; Ko, D.C.K.; Cheung, C.W.; Porter, J.F.; McKay, G. (2004) Film and intraparticle mass transfer during the adsorption of metal ions onto bone char. *J. Colloid and Interface Sci*, *271*: 284.
30. Benguella, B.; Benaissa, H. (2002) Cadmium removal from aqueous solutions by chitin: kinetic and equilibrium studies. *Water Res.*, *36*: 2463.
31. Cheung, C.W.; Chan, C.K.; Porter, J.F.; McKay, G. (2001) Film-pore diffusion control for the batch sorption of cadmium ions from effluent onto bone char. *J. Colloid Interface Sci.*, *234*: 328.
32. Cheung, C.W.; Porter, J.F.; McKay, G. (2002) Removal of Cu(II) and Zn(II) ions by sorption onto bone char using batch agitation. *Langmuir*, *18*: 650.
33. Levinskas, G.J.; Neuman, W.F. (1955) The solubility of bone mineral. I. Solubility studies of synthetic hydroxylapatite. *J. Phys. Chem.*, *59*: 164.
34. Lagergren, S. (1898) Zur theorie der sogenannten adsorption geloster stoffe, Kungliga Svenska Vetenskapsakademiens. *Handlingar*, *24*: 1.
35. Ho, Y.S.; McKay, G. (1999) Pseudo-second order model for sorption processes. *Process Biochem.*, *34*: 451.

36. Weber, W.J.; Morris, J.C. (1963) Kinetics of adsorption on carbon from solution. *J. Sanit. Eng. Div. Am. Soc. Civ. Eng.*, *89*: 31.
37. Hameed, B.H.; El-Khaiary, M.I. (2008) Sorption kinetics and isotherm studies of a cationic dye using agricultural waste: Broad bean peels. *J. Hazard. Mater.*, *154*: 639.
38. Chen, C.; Wang, J. (2008) Removal of Pb^{2+}, Ag^{+}, Cs^{+} and Sr^{2+} from aqueous solution by brewery's waste biomass. *J. Hazard. Mater.*, *151*: 65.
39. Chojnacka, K. (2004) Equilibrium and kinetic modeling of chromium (III) sorption by animal bones. *Chemosphere*, *59*: 315.
40. Bektas, N.; Kara, S. (2004) Removal of lead from aqueous solutions by natural clinoptilolite: equilibrium and kinetic studies. *Sep. Purif. Technol.*, *39*: 189.
41. Saxena, S.; Prasad, M.; D'Souza, S.F. (2006) Radionuclide sorption onto low-cost mineral adsorbent. *Ind. Eng. Chem. Res.*, *45*: 9122.
42. Ozacar, M.; Sengil, I.A. (2004) Application of kinetic models to the sorption of disperse dyes onto alunite. *Colloids and Surfaces A*, *242*: 105.
43. Ofomaja, A.E. (2007) Kinetics and mechanism of methylene blue sorption onto palm kernel fibre. *Process Biochem.*, *42*: 16.
44. Ofomaja, A.E. (2008) Sorptive removal of methylene blue from aqueous solution using palm kernel fibre: Effect of fibre dose. *Biochem. Eng. J.*, *40*: 8.